Measurement Science
and Technology

100 year anniversary
Measurement Science and Technology

PURPOSE-LED
PUBLISHING™

PAPER • OPEN ACCESS

Calibration and validation of a bleeding detector for beveled PMMA applicators in electron intraoperative radiotherapy

To cite this article: Rafael Garcia-Gil *et al* 2024 *Meas. Sci. Technol.* **35** 085115

OPEN ACCESS
IOP Publishing
Measurement Science and Technology
Meas. Sci. Technol. **35** (2024) 085115 (9pp)
https://doi.org/10.1088/1361-6501/ad48a6

Calibration and validation of a bleeding detector for beveled PMMA applicators in electron intraoperative radiotherapy

Rafael Garcia-Gil[1], **Silvia Casans**[1], **A Edith Navarro-Antón**[1,*], **Julio Martos**[1], **Malamati Giompliaki**[1], **Ignacio Pérez-Calatayud**[1], **Enrique Sanchis**[1,2], **José Pérez-Calatayud**[2,3,4] **and Enrique Sanchis-Sánchez**[5]

[1] Department of Electronic Engineering, University of Valencia, Burjassot, Spain
[2] IRIMED Joint Research Unit IIS La Fe—University of Valencia, Valencia, Spain
[3] Department of Radiation Oncology, La Fe Hospital, Valencia, Spain
[4] Department of Radiation Oncology, Clínica Benidorm, Alicante, Spain
[5] Department of Physical Therapy, University of Valencia, Valencia, Spain

E-mail: enavarro@uv.es

Received 18 December 2023, revised 3 May 2024
Accepted for publication 8 May 2024
Published 17 May 2024

CrossMark

Abstract

This study aimed to calibrate and validate a capacitive-sensor bleeding detector, originally designed for flat applicators, with beveled applicators (bPMMA), which are among the most commonly used applicators in intraoperative radiotherapy with electron mobile linacs. The detector will help prevent dose misadministration during irradiation in the event of fluid accumulation in the applicator, thus allowing for appropriate intervention. The handicap with employing this detector for bPMMA stems from the fact that the level of accumulated fluid depends on both the tilting angle and orientation of the applicator. Furthermore, the fluid remains accumulated at the bottom corner of the applicator, reducing the sensitivity of the sensor. A 5-strip capacitive sensor has been used, attached to a 4 cm diameter 30° beveled applicator with a tilting angle range from 0° to 30°. The sensor is read out using dedicated electronics, including a Wheatstone bridge circuit, amplifier, filter stages, and microcontroller. To calculate the sensitivity of the sensor, a prior calibration of the circuit has been carried out in order to obtain the relationship between the output voltage of the conditioning circuit and the height of the fluid present in the applicator for different inclinations. Using the average sensitivity over the inclination range of interest can provide accurate measurements of the estimated fluid height up to 12 mm, with a maximum deviation of approximately 2.0 mm and less than 1.0 mm for the 5 mm clinic threshold. The use of the mean sensitivity is a practical approach for detecting bleeding in beveled applicators because it simplifies the measurement process by avoiding the need to obtain detector sensitivity for each inclination and orientation of the applicator, which would be complex if not impractical in clinical use.

Keywords: intraoperative radiotherapy, mobile linac, beveled applicator, capacitive-based bleeding detector

[*] Author to whom any correspondence should be addressed.

1. Introduction

Intraoperative electron radiotherapy (IOERT) is a technique that is gaining popularity because of advancements in portable electron linear accelerators with sufficient self-shielding capabilities [1]. This allows IOERT to be used in conventional operating rooms, which make it a convenient option for patients. IOERT can be used to treat a variety of diseases, either as a standalone therapy or in combination with external radiotherapy. This versatility makes IOERT a relevant and cutting-edge option in the field of radiotherapy [2–7]. The recent developments in electron therapy and IOERT, in particular, have generated significant excitement in the radiation therapy community due to the imminent availability of portable electron devices that can perform FLASH-type treatments [8].

Treatments can be delivered using flat (fPMMA) or beveled (bPMMA) applicators [9]. These applicators are used not only in conventional operating rooms without special wall shielding, but also in situations where it is crucial to neutralize the required roll and pitch angle of the beam by bringing it closer to the vertical direction. In these situations, bPMMA applicators are better adapted to inclined surfaces and ensure that the tumor or tumor bed is in full contact with the applicator tip, leading to a more homogeneous dose distribution. In addition, the bevel is essential to adapt to the surgical bed and ensure optimal contact with the access tissue, especially in the case of deep targets, thus avoiding any gaps in the treatment. Its use is also motivated by the need for the linac gantry to be as close as possible to the vertical for reasons of radiological protection. In particular, the beam must always be directed towards the floor, where the beam stopper is located (the beam stopper ensures protection of the rooms below the operating room, where the irradiation takes place). Figure 1 shows the use of a bPMMA applicator in clinical practice.

Useful inclinations in clinical practice include the range between 0° and 30°, measured with respect to the vertical plane. According to data collected at Hospital La Fe in Valencia, Spain, 77% of the treatments for the 103 patients treated required the use of bevels, specifically 15° (33%), 30° (25%), and 45° (19%).

One of the potential risks that can cause dose misadministration during irradiation is the potential bleeding in the tumor bed [3]. This is especially problematic in highly vascularized situations or when organic fluids are presents [9]. This unwanted clinical circumstance currently has no solution, which implies a potential deviation from the ideal clinical treatment. In practice, an attempt is made to avoid this circumstance by orienting the applicator favoring its evacuation or very frequent suctions. This procedure clearly does not guarantee the absolute security of this disturbance.

Due to the high gradient of direct electron fields after their therapeutic range (Rt), the existence of unexpected fluid altering the planned depth may result in underdose of the treatment volume.

The prescription depth is usually set close to the Rt of the electrons, which corresponds to the 90% depth of the percent depth curve. This depth varies with the energy of the electrons but is also influenced by the bevel angle of the applicator. Beyond Rt, the dose decreases appreciably in a gradient that increases with decreasing energy. Most treatments are performed on surgical beds primarily for prophylactic purposes. Therefore, the smallest available prescription depth, typically ranging between 1 and 1.5 cm, is often used. Occasionally, irregularities or protrusions in the tissue being treated may necessitate adjustments to the prescription depth. As a safety precaution, an increase in the prescription depth of at least 5 mm is usually considered in clinical practice.

Figure 1. Arm sarcoma intervention using a 6 cm diameter 30° beveled applicator.

The use of a bleeding detector can help prevent dose misadministration during irradiation by detecting the presence of bleeding and allowing for appropriate intervention if a fluid threshold is exceeded in the applicator. The potential bleeding to be controlled with the proposed detector occurs from the moment the applicator is fully attached (hard-docking) until irradiation.

The use of detectors to measure the presence of fluid in a recipient is common in fields such as in industrial, medical or environmental monitoring applications [10–13]. Although bleeding detectors for medical applications can be found in the literature [14–17], the problem of real-time bleeding detection in IOERT treatments has only been found in [18–20]. Bleeding detectors described in [14–17] basically perform the detection through image processing [14–16] or augmented reality and processing through artificial intelligence [17]. However, none of these works specify the accumulated fluid height that is required in this application.

Designing a fluid level detector for IOERT indeed poses a challenge due to stringent regulatory standards mandating the avoidance of direct contact between the detector and the patient. This requires placing the detector outside the applicator, which results in a 5 mm gap between the sensor and the fluid, equivalent to the thickness of the applicator.

Detecting liquid levels as low as 5 mm under such restrictive conditions is a technical novelty that presents several challenges, including: (1) *Sensitivity*, the detector must be highly sensitive to detect small changes in capacitance associated with fluid level variations within the very narrow 5 mm range; (2) *Accuracy*, the detector must provide accurate measurements despite the limited separation distance, ensuring that even extremely low variations in fluid level are reliably detected; (3) *Interference reduction*, external factors such as ambient noise or electromagnetic interference can affect detector performance, requiring the use of shielding and noise reduction techniques; (4) *Calibration,* the detector must be calibrated very accurately to account for factors such as variations introduced by external placement of the sensor as well as other restrictive conditions associated with its clinical use; (5) *Safety*, it is essential to ensure that the operation of the detector does not pose any risk to the patient, which requires considerations such as electrical safety and compatibility with the IOERT procedure.

A bleeding detector for flat translucent polymethyl methacrylate applicators (PMMA) has been proposed by Sanchis *et al* [18, 19], and García-Gil *et al* [20, 21], where a threshold for fluid detection of 5 mm was considered according to Gunderson *et al* [1]. The dosimetric effects of adding 5 mm to the Rt depend on both the energy and the bevel used. The significance of this effect decreases when increasing electron energies. Another reason for choosing this value of 5 mm is because it is the minimum safety increment used to add to the prescription depth in our hospital.

In these papers, the feasibility of bleeding detector for fPMMA applicators has been thoroughly explored. The detector consists of a capacitive sensor, its associated readout electronics and a wireless power supply. It is embedded in the fPMMA applicator so that there is no contact with the patient and eliminates any dependence on the accelerator. The detector incorporates a mobile application that allows the surgical team to verify the presence of accumulated fluid in the applicator both before and during the irradiation process. The solution proposed by García-Gil *et al* [20] for fPMMA applicators meets all clinical requirements: 5 mm detection capability, high visibility, no patient contact, linac independence, no interference with the irradiation beam and easy-to-use. Nevertheless, the bleeding detection solution for bPMMA applicators has not yet been solved, despite these being the most widely used clinically.

In the case of the bPMMA applicators under study, the complexity of the problem increases due to the particular geometry of the capacitive sensor-applicator assembly. This specific geometry implies that the capacitance variations for bPMMA applicators must be detected at levels well below the 0.1 pF typically measured for fPMMA applicators with the previously designed detector. This indicates a high level of sensitivity and accuracy needed to detect capacitance variations in bPMMA applicators.

The aim of this work is to investigate the feasibility and perform the characterization of a capacitive sensor-based bleeding detector, previously developed for flat applicators [18–21], for use with beveled applicators. The challenge regarding the use of this detector for beveled applicators lies in the fact that: (1) the height of the accumulated fluid depends not only on the tilting angle of the applicator but also on its orientation; (2) there is no analytical expression to obtain the height of the accumulated fluid in the applicator based on its volume, considering both the tilting angle and orientation; (3) the sensitivity of the sensor also depends on the tilting angle and orientation of the applicator; (4) the fluid remains accumulated at the corner of the applicator, reducing the sensitivity of the sensor. The final orientation of the plane at the end of the applicator is determined by both the rotation of the arm of the accelerator and the orientation of the bevel. Therefore, the level of the fluid with respect to the end of the applicator is highly variable, between a layer parallel to it to a local accumulation at its extreme tip.

We highlight the relevance of the present work in a measurement context in the following issues: (1) The design of the sensor surrounding a circular bPMMA applicator with minimal visual impact, while maintaining adequate sensing capability; (2) The procedure to obtain the accumulated fluid height in a bPMMA applicator for different orientations and inclinations, based on simulations using AutoCAD; (3) The study of the sensor sensitivity and its associated error for different orientations and inclinations of bPMMA applicators.

This paper is organized as follows. section 2.1 presents the mobile linac and the beveled applicator (bPMMA) on which the bleeding detector (capacitive sensor and conditioning circuit) is embedded. The electronics of the bleeding detector is described in sections 2.2 and 2.3 shows the setup used to obtain the calibration curves (voltage vs fluid height) of the bleeding detector for different inclinations. Inclinations (0°–30° from the vertical plane) are generated by rotating the orientation of the bevel plane a 90° quadrant. A previous study of the relationship between the volume of fluid added to the applicator and its corresponding height measured on the wall of the applicator, needed for calibration, is carried out through simulation with AutoCAD and extrapolation to different orientations. Section 3 outlines the experimental results, including the measurement of sensor sensitivity in mm V^{-1} for different orientations and the deviation in the fluid height estimated that occurs when considering a constant sensitivity for all orientations. In section 4 a brief discussion takes place, while in section 5 conclusions are drawn.

2. Materials and methods

2.1. Mobile linac and beveled applicator

The LIAC HWL Mobile linac [20, 22] offers electron energies at 6, 8, 10, and 12 MeV. To enable direct visualization of the tumor bed, PMMA applicators are used. The diameters of these applicators range from 3 cm to 12 cm with terminal bevel angles ranging from 0° to 45°. Typically comprising two pieces, the upper part is affixed to the linac head and the lower piece is in contact with the patient. The hard-docking mechanism employs toggle latches that firmly connect these two pieces. The typical radiation treatment lasts less than two minutes and delivers doses of up to 20 Gy. The dose per pulse with a 10 cm diameter applicator can range from approximately 1–8 cGy p^{-1}, and the corresponding dose rate can be set from 10 to 30 Gy min^{-1}, depending on the energy used. These parameters provide a flexible and efficient system for delivering targeted radiation therapy during surgery [22].

The portable electron linear accelerator used in IOERT has been designed to minimize parasitic radiation (stray radiation, SR) so that it can be used in a conventional operating room without additional shielding. This is achieved by using an optical system that reduces the interaction between the accelerated electron beam and any metallic element, resulting in a minimal global SR of 0.2 µSv Gy^{-1} in the patient plane at a distance of 3 m from the target [22]. This reduction in SR allows for maximum utilization of the equipment. A previous study [20] showed that there were no variations in SR measurements made with both standard and instrumented applicators (equipped with an embedded bleeding detector), thus maintaining the excellent SR performance of the linac.

A 4 cm diameter 30° beveled translucent polymethyl methacrylate applicator (bPMMA) from Sordina IORT Technologies [22] has been considered in this work. This applicator diameter is critical from the point of view of bleeding detection among those highly used in the clinic. The 30° bevel bPMMA is the mostly used in clinical practice.

2.2. Sensor and read-out electronics

The bleeding detector used in this paper is based on a capacitive sensor as described by Garcia-Gil *et al* [19]and on an electronic conditioning circuit that utilizes an AC-Wheatstone bridge as described by García-Gil *et al* [21] .

The capacitive sensor was modified to adapt to the bPMMA applicator by designing it to follow the perimeter of the ellipsoidal end of the applicator, as shown in figure 2. The sensor is composed of two capacitive plates (top and bottom), each made up of a set of sandwiched strips that are 15 mm in height. A 5-strip capacitive sensor was used, which achieves an increased visual field of 10% compared to the 6-strip sensor used in previous publications [18–20], but at the cost of reduced sensor sensitivity.

The presence of fluid in the applicator modifies the dielectric constant and, therefore, the value of its equivalent capacity C_x (figure 3). This capacitance variation is measured by the

Figure 2. View of the capacitive sensor deployed to be adapted to the bPMMA applicator. The sensor geometry follows the perimeter of the ellipsoidal end of the applicator.

AC-Bridge, where the AC source is generated by a Wien oscillator with an oscillation frequency of 20 kHz. The AC-Bridge is composed of the capacitor sensor (C_x), a potentiometer (R_x) for bridge balancing and a reference resistor–capacitance (R_o–C_o). C_o eliminates the bias source introduced by both the capacitance of the bifilar cable and the sensor capacitance when there is no fluid in the applicator (zero condition). R_o has been taken to fix a cut-off frequency of the R_o–C_o voltage divider below the 20 kHz working frequency. The resulting AC signal (v_d) is amplified by an instrumentation amplifier (IA) integrated circuit (figure 3). Since the capacitance changes to be measured are very small (less than 0.1 pF) significant amplification is required (gain of 50). The output signal (V_o) is obtained after being rectified, filtered and finally digitized by a microcontroller. This voltage is proportional to the level of fluid inside the applicator. From calibration it is possible establish the correlation between the voltage provided by the conditioning circuit (V_o) and the fluid height within the applicator. The calibration procedure is shown in section 3, where the sensitivity of the sensor to be programmed in the microcontroller is obtained. The microcontroller is equipped with an accelerometer, which measures the angle of inclination of the applicator. This feature is useful for verifying that the applicator is within the operating range of 0°–30°, measured respect to the vertical plane. Data is finally sent via USB port to a PC and graphically represented by a developed LabVIEW-based graphical interface.

The proposed bleeding detector is conceived to operate independently of the accelerator, but could potentially be integrated into it to improve safety and efficiency during radiation therapy treatments.

2.3. Setup for measuring the detector sensitivity and calibration

Tests have been conducted using water as the equivalent of blood or any organic fluid present in the applicator. Water has been introduced into the bPMMA applicator by using the commercial 7PV1000 pipettor (min. 200 µl, 5 µl resolution) from Bibby Sterilin Ltd. Figure 4 shows the bPMMA applicator and the read-out electronics. To obtain the detector sensitivity, it is necessary to previously establish the relationship between the volume of fluid added to the applicator and its corresponding

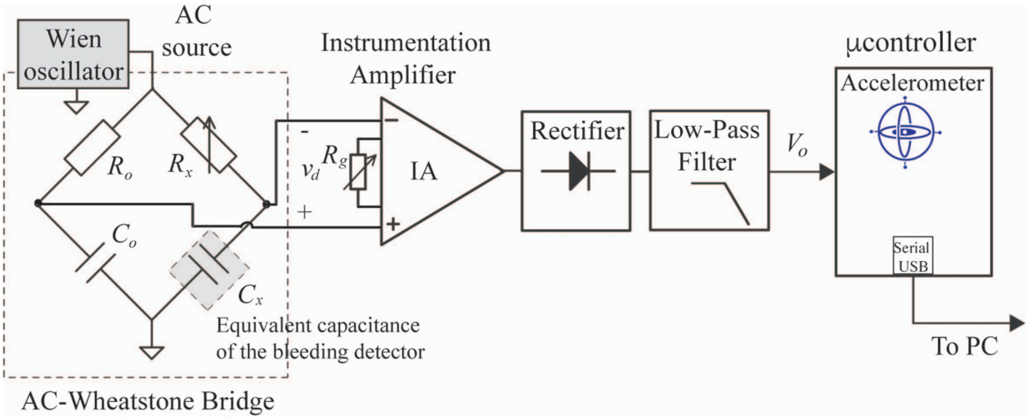

Figure 3. Read-out circuit block diagram.

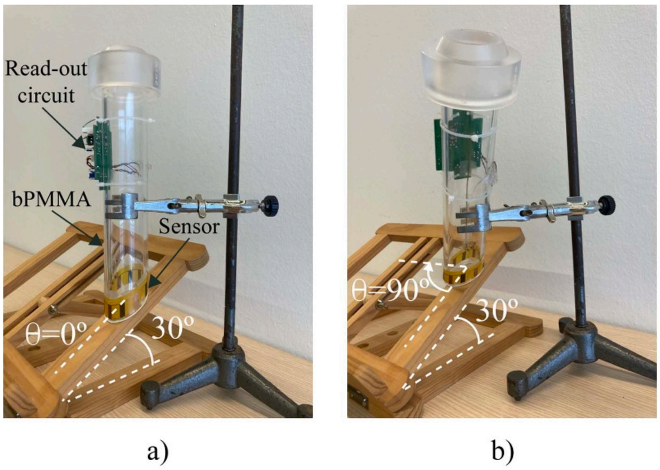

Figure 4. Setup for measuring the detector sensitivity and calibration. (a) Effective inclination of 0° (0° orientation), (b) effective inclination of 30° (90° orientation).

height measured on the wall of the applicator. In contrast to flat applicators, in the case of beveled applicators this relationship can be challenging to determine, depending on the angle formed by the base of the applicator with the horizontal plane (which varies with the inclinations of the applicator).

The experimental setup shown in figure 4 tilts the applicator 30° from the horizontal plane. The most frequent tilting angles (0°–30° from the vertical plane) are generated by rotating the orientation of the bevel plane a 90° quadrant. The position of the beveled applicator in which the major axis of the ellipse coincides with the inclined plane generates 0° inclination (vertical, figure 4(a)), while rotating the orientation of the bevel plane from this position to a 90° quadrant generates effective tilts of the applicator axis to 30° from vertical (figure 4(b)). To summarize, when the bPMMA applicator is tilted 30° from the horizontal plane, the effective inclination of 0° is obtained for an orientation of 0° (as shown in figure 4(a)) and an effective inclination of 30° is obtained for an orientation of 90° (as shown in figure 4(b)), both with respect to the major axis of the ellipse. This study has only considered 0° and 90° orientations due to their clinical relevance (i.e. they generate 0° and 30° effective tilting angles, respectively), but it could be extended to include other values if necessary.

A total of 60 calibrations were carried out, with 10 calibrations for 6 different orientations between 0° and 90° (0°, 10°, 35°, 50°, 80°, 90°). At least 12 points were acquired for each calibration process, with each point corresponding to the average of 10 measurements. Data was collected using a custom LabVIEW-based monitoring application that was previously developed [19, 21].

The 30° angle formed by the base of the applicator with respect to the horizontal plane complicates establishing a direct relationship between the volume (V in ml) and height of the fluid (h in mm), as the fluid will accumulate in one corner of the applicator, and this relationship depends on the orientation of the applicator. To obtain this relationship for different orientations, simulation with AutoCAD software was used. Figure 5(a) shows AutoCAD results for 0° orientation (i.e. 0° applicator tilting angle), in which the major axis of the ellipse coincides with the area of maximum fluid accumulation, and figure 5(b) the AutoCAD results for 90° orientation. In general, for any orientation, points can be fitted to a potential equation,

$$h = A \cdot V^{B} \tag{1}$$

where A and B are orientation-dependent parameters. Figure 6 shows the variation of these parameters for different orientations (θ in equation (2)).

As shown in figure 6, parameter A can be fitted to a linear expression, while parameter B can be considered approximately constant,

$$\begin{aligned} A &= -0.035 \cdot \theta + 11.495 \\ B &= 0.407. \end{aligned} \tag{2}$$

3. Results

Figure 7 shows the dependence of the detector sensitivity with the orientation angle, which was derived from analyzing a set

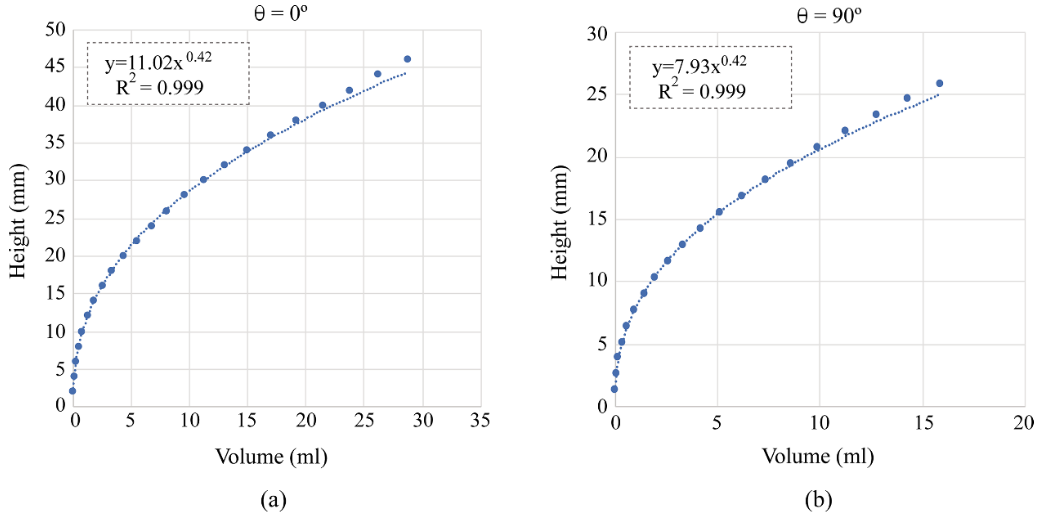

Figure 5. Maximum height vs volume dependence from AutoCAD simulation for: (a) 0° orientation (0° applicator tilting angle); (b) 90° orientation (30° applicator tilting angle).

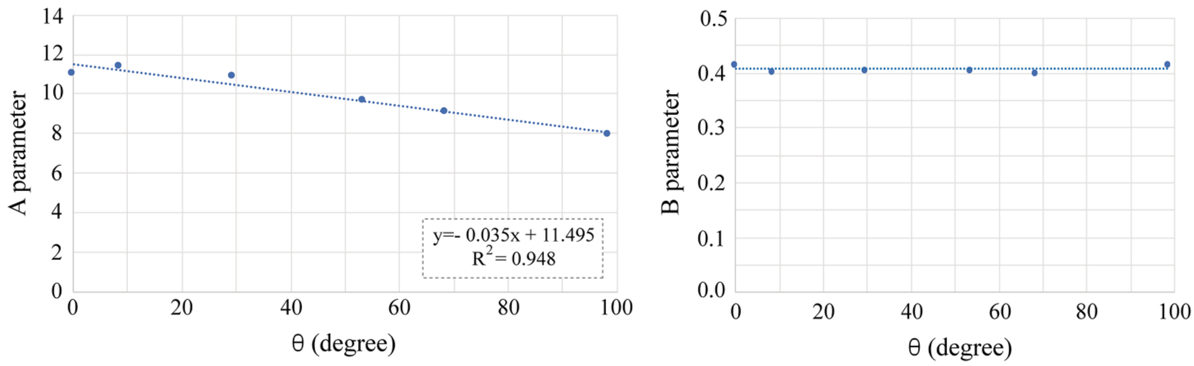

Figure 6. Parameters (A) (left) and (B) (right) as a function of the orientation.

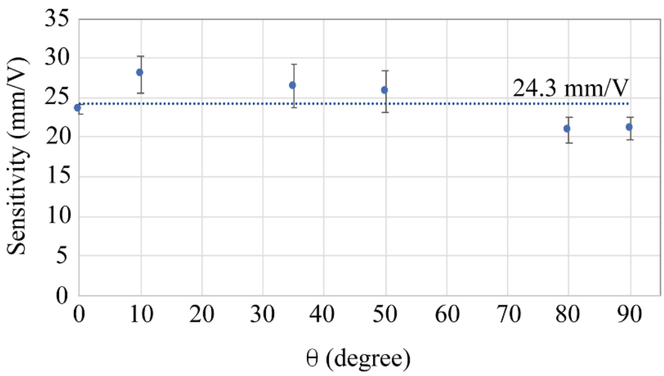

Figure 7. Sensor sensitivity as a function of orientation.

of calibration measurements (V_o vs h). The sensitivity of the detector to estimate the fluid height was determined by averaging the sensitivities obtained in the 6 orientations considered in the experimental study (from 0° to 90°), resulting in a value of 24.3 mm V^{-1}.

Figure 8 shows the complete set of data obtained for fluid height estimates for each of the 6 orientations previously analyzed, and for actual fluid heights up to 12 mm. Each point in the graph represents the mean value of estimated fluid height for each actual height and orientation considered, and the error bars represent its associated uncertainty. Knowing the volume of fluid introduced into the applicator, the current height has been calculated using equations (1) and (2). For the height estimation made by the system, a fixed sensitivity of 24.3 mm V^{-1} has been considered. The maximum deviation from the bisecting line, considered as the ideal detector response, is approximately 2.0 mm for the entire 12 mm height range and less than 1.0 mm for the 5 mm threshold (figure 8). The greatest uncertainty occurs for an orientation near 90°, which corresponds to an effective tilting angle of 30° (less common in clinical practice than an effective tilting angle of 0°). The variability in the mean uncertainty values is caused by the differences in uncertainties for different orientations when a mean sensitivity value is used instead of the actual value.

4. Discussion

The use of bPMMA applicators allows a near-vertical orientation of the gantry which allows the efficient use of the beam-stopper because the floor is the primary barrier, ensuring the safe administration of the radiation dose. Additionally,

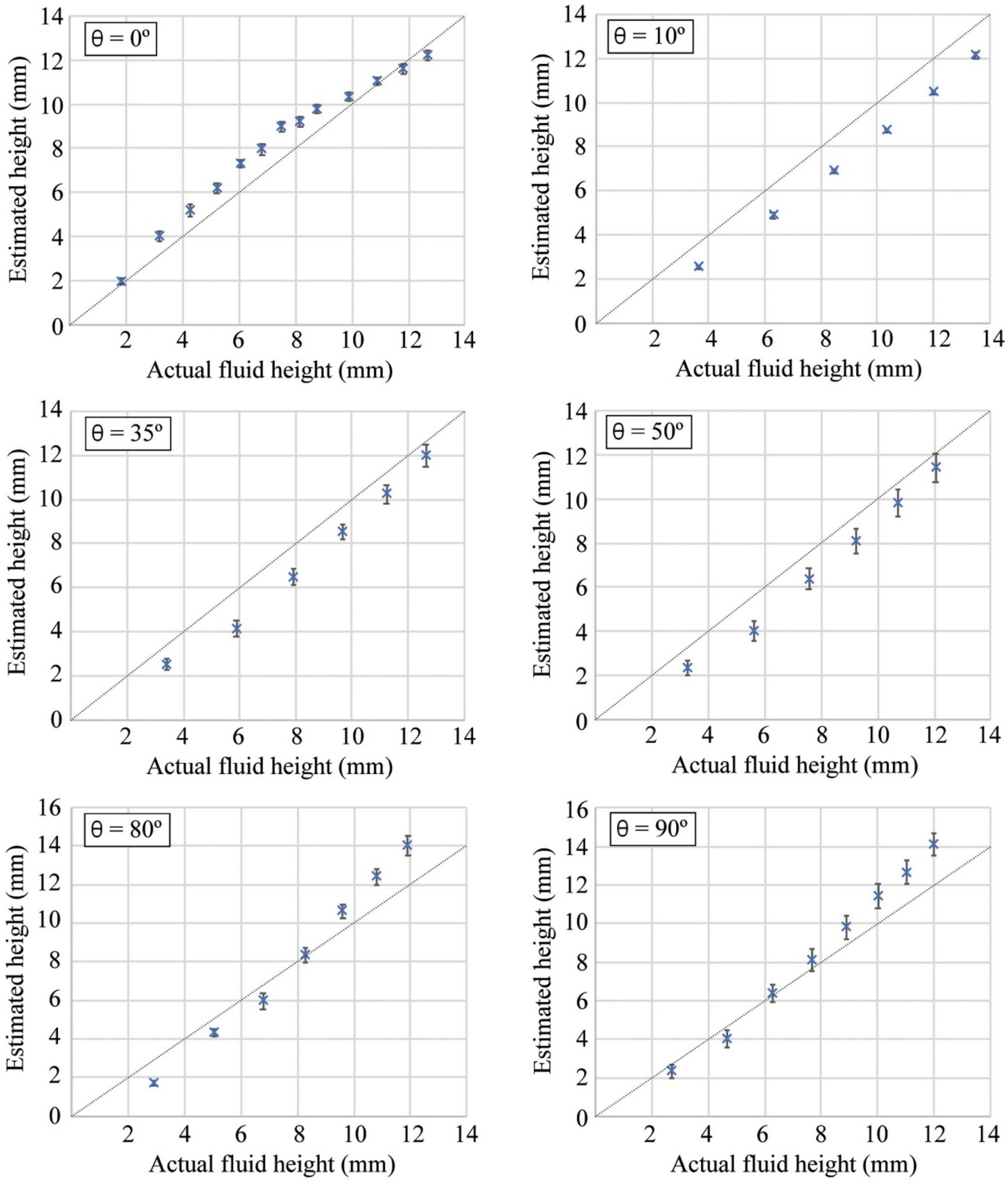

Figure 8. Estimated fluid height vs actual height for different orientations. The dashed line represents the idealized response of the detector, which is the bisector of the graph. Error bars represent one standard deviation.

the beveled applicator can better adapt in most cases to the surface of the treatment area, providing a more homogeneous dose distribution and improving treatment effectiveness.

The study evaluated the ratio between estimated height and actual height for inclinations of the applicator ranging from 0° to 30°, measured with respect to the vertical plane, which are relevant for clinical practice. These inclinations were obtained with the base of the applicator inclined 30° from the horizontal plane, rotating its base a 90° quadrant (between 0° and 90° respectively), as shown in figure 4.

To establish the relationship between fluid volume and height within the applicator, we conducted simulations using AutoCAD, obtaining equations (1) and (2). These equations enable us to extrapolate the results for any orientation of the applicator.

We have estimated the height of the accumulated fluid in the applicator up to 12 mm, and a fixed sensitivity of 24.3 mm V^{-1} was assumed for the selected 6 orientations of the applicator (effective tilting angles of the applicator in the range of 0°–30°). Values close to the maximum height of the sensor (15 mm) showed a poorer response due to the effective dielectric constant of the sensor-air interface and were therefore discarded, but this did not affect the detection of the 5 mm threshold.

As can be seen in figure 7, the sensitivity of the sensor is worse in the case of orientations close to 10° because the liquid accumulates in the corner of the applicator, as happened with the bleeding detector for fPMMA presented in [20].

After assuming a constant sensitivity for all orientations, figure 8 shows how the estimation of the height of the fluid made by the system varies with this orientation. The maximum deviation from ideal response was approximately 2.0 mm for the entire range and less than 1.0 mm for the 5 mm threshold. The greatest uncertainty occurred for an orientation of 90°, which corresponds to an effective tilting angle of 30°, although this is less common than 0° in clinical practice. Despite the bPMMA applicator having a greater maximum deviation in the estimation of the height of the fluid compared to flat PMMA applicators, it still meets the clinical requirement of detecting the 5 mm threshold.

The deviations in height estimation could be reduced by obtaining sensitivity as a function of inclination and orientation, as was done by García-Gil *et al* [20] for flat applicators, but this would be a more complex process in the case of bPMMA applicators and may not be viable. Moreover, such a complex process is not necessary for clinical purposes, as the main objective is to detect a fluid level greater than 5 mm.

The limitations of this study include the use of only one specific applicator (4 cm, 30° bevel) and a limited range of inclinations (between 0° and 30°), which are mostly used in the clinic. Therefore, further studies would be necessary to determine the sensitivity mean value for each geometry of the bPMMA applicator (i.e. different diameters and bevels) to generalize the use of the detector in a clinical environment.

In our hospital's experience, hard-docking usually lasts between 5 and 10 min, while irradiation lasts between 1 and 2 min (typical doses range between 12 and 21 Gy). In our clinical practice no cases of blood coagulation have been detected that could hypothetically alter the detector response.

5. Conclusions

This study has confirmed the feasibility of using a capacitive-based bleeding detector previously designed for flat PMMA applicators to detect bleeding in bPMMA applicators, most commonly used in radiotherapy.

The use of the average sensitivity over the range of inclinations of interest (0°–30°, measured from the vertical plane) can provide accurate measurements of the estimated fluid height up to 12 mm, with a maximum deviation of approximately 2.0 mm and less than 1.0 mm for the 5 mm threshold. Although considering a fixed sensitivity has limitations in accuracy, it greatly simplifies the measurement process by avoiding the need to obtain detector sensitivity for each inclination and orientation of the applicator, which would be complex if not impractical in clinical use.

The deviation in fluid height estimation resulting from the comparison with the idealized response of the detector allows for the detection of the required 5.0 mm yes/no threshold in a clinical setting, validating the use of the bleeding detector with the beveled applicator.

Data availability statement

All data that support the findings of this study are included within the article (and any supplementary files).

Acknowledgments

This work is framed in a previous collaboration agreement between S I T Sordina IORT Technologies SpA and University of València-Estudi General.

We would like to thank Mr Julio Martos (jr) for his valuable contributions during simulation tasks and Professor Javier Vijande for his assistance with data representation.

Funding

Authors declare that no funds, grants, or other support were received during the preparation of this manuscript.

Conflict of interest

Authors declare no conflicts of interest.

Ethics statement

No ethical statement is required in this study.

ORCID iDs

Rafael Garcia-Gil https://orcid.org/0000-0002-9215-5362
A Edith Navarro-Antón https://orcid.org/0000-0003-4663-8547
Enrique Sanchis-Sánchez https://orcid.org/0000-0002-3781-2083

References

[1] Gunderson L L, Willett C G, Calvo F A and Harrison L 2011 Intraoperative Irradiation *Techniques and Results* (Springer)

[2] Beddar A S, Biggs P J, Chang S, Ezzell G A, Faddegon B A, Hensley F W and Mills M D 2006 Intraoperative radiation therapy using mobile electron linear accelerators; Report of the AAPM Radiation Therapy Committee Task Group No. 72 *Med. Phys.* **12** 1476–89

[3] Calvo F A 2017 Intraoperative irradiation: precision medicine for quality cancer control promotion *Radiat. Oncol.* **12** 1–5

[4] Haddock M G 2017 Intraoperative radiation therapy for colon and rectal cancers: a clinical review *Radiat. Oncol.* **12** 1–8

[5] Roeder F and Krempien R 2017 Intraoperative radiation therapy (IORT) in soft-tissue sarcoma *Radiat. Oncol.* **12** 1–13

[6] Krengli M, Pisani C, Deantonio L, Surico D, Volpe A, Surico N and Terrone C 2017 Intraoperative radiotherapy in gynaecological and genito-urinary malignancies: focus on endometrial, cervical, renal, bladder and prostate cancers *Radiat. Oncol.* **12** 18

[7] Calvo F A, Sole C V, Rutten H J, Poortmans P, Asencio J M, Serrano J, Aristu J, Roeder F and Dries W J 2020 ESTRO/ACROP IORT recommendations for intraoperative radiation therapy in primary locally advanced rectal cancer *Clin. Transl. Radiat. Oncol.* **25** 29–36

[8] Felici G *et al* 2020 Transforming an IORT linac into a FLASH research machine: procedure and dosimetric characterization *Front. Phys.* **8** 1–11

[9] López-Tarjuelo J, Morillo-Macías V, Bouché-Babiloni A, Ferrer-Albiach C and Santos-Serra A 2015 Defining action levels for in vivo dosimetry in intraoperative electron radiotherapy *Technol. Cancer Res. Treat.* **15** 453–9
[10] Timaeus R, Berger R, Schleicher E, Hampel U and Schubert M 2019 Liquid flow visualization in packed-bed multiphase reactors: wire-mesh sensor design and data analysis for rotating fixed beds *Chem. Ing. Tech.* **91** 1812–21
[11] Chen W, Huang J, Zhu C, Xu F and Huang Q A 2019 An interdigital capacitive humidity sensor with layered black phosphorus flakes as a sensing material *IEEE Sens. J.* **19** 11007–13
[12] de Gioia S, Adamo F, Attivissimo F, Lotano D and Di Nisio A 2023 A design strategy for performance improvement of capacitive sensors for in-flight oil-level monitoring aboard helicopters *Measurement* **208** 112476
[13] Loizou K and Koutroulis E 2016 Water level sensing: state of the art review and performance evaluation of a low-cost measurement system *Measurement* **89** 204–14
[14] Tang J *et al* 2022 Bleeding contour detection for craniotomy *Biomed. Signal Process. Control* **73** 103419
[15] Xu H *et al* 2022 Detection of blood stains using computer vision-based algorithms and their association with postoperative outcomes in thoracoscopic lobectomies *Eur. J. Cardiothorac. Surg.* **62** ezac154
[16] Checcucci E *et al* 2023 Development of bleeding artificial intelligence detector (BLAIR) system for robotic radical prostatectomy *J. Clin. Med.* **12** 7355
[17] Rus G, Andras I, Vaida C, Crisan N, Gherman B, Radu C, Tucan P, Iakab S, Hajjar N A and Pisla D 2023 Artificial intelligence-based hazard detection in robotic-assisted single-incision oncologic surgery *Cancers* **15** 3387
[18] Sanchis E, Casans S, Felici G, García-Gil R, Sanchis-Sánchez E, Pérez-Calatayud I, Pérez-Calatayud M J and Pérez-Calatayud J 2019 Detector for monitoring potential bleeding during electron intraoperative radiotherapy *Phys. Med.* **57** 95–99
[19] Sanchis E, Casans S, García-Gil R, Martos J, Sanchis-Sánchez E, Pérez-Calatayud I, José Pérez-Calatayud M and Pérez-Calatayud J 2019 Improving bleeding detector features for electron intraoperative radiotherapy *Phys. Med.* **65** 150–6
[20] Garcia-Gil R, Casans S, Edith Navarro A, García-Sánchez A J, Rovira-Escutia J J, Garcia-Costa D, Sanchis-Sánchez E, Pérez-Calatayud I, Pérez-Calatayud J and Sanchis E 2022 Embedded bleeding detector into a PMMA applicator for electron intraoperative radiotherapy *Phys. Med.* **94** 35–42
[21] Garcia-Gil R, Casans Berga S, Sanchis-Sanchez E, Perez-Calatayud I, Perez-Calatayud J and Sanchis Peris E 2021 Electronic design for a bleeding detector to be used in intraoperative radiotherapy applications *IEEE Sens. J.* **21** 4786–92
[22] Sordina IORT Technologies LIACHWL Mobile IOeRT Accelerator (available at: www.soiort.com)